ResearchGate

See discussions, stats, and author profiles for this publication at: https://www.researchgate.net/publication/225291660

Self-Assembled Peptide Nanotubes as an Etching Material for the Rapid Fabrication of Silicon Wires

ARTICLE *in* BIONANOSCIENCE · JUNE 2011

DOI: 10.1007/s12668-011-0005-6

CITATIONS
10

READS
28

4 AUTHORS, INCLUDING:

Karsten B Andersen
Technical University of Denmark
13 PUBLICATIONS **93** CITATIONS

SEE PROFILE

Winnie E Svendsen
Technical University of Denmark
114 PUBLICATIONS **1,390** CITATIONS

SEE PROFILE

Jaime Castillo-Leon
Sol Voltaics AB, Lund, Sweden
44 PUBLICATIONS **654** CITATIONS

SEE PROFILE

Available from: Jaime Castillo-Leon
Retrieved on: 24 January 2016

BioNanoSci. (2011) 1:31–37
DOI 10.1007/s12668-011-0005-6

Self-Assembled Peptide Nanotubes as an Etching Material for the Rapid Fabrication of Silicon Wires

Martin B. Larsen · Karsten B. Andersen · Winnie E. Svendsen · Jaime Castillo-León

Published online: 26 April 2011
© Springer Science+Business Media, LLC 2011

Abstract This study has evaluated self-assembled peptide nanotubes (PNTS) and nanowires (PNWS) as etching mask materials for the rapid and low-cost fabrication of silicon wires using reactive ion etching (RIE). The self-assembled peptide structures were fabricated under mild conditions and positioned on clean silicon wafers, after which these biological nanostructures were exposed to an RIE etching process. Following this treatment, the structure of the remaining nanotubes and nanowires was analyzed by scanning electron microscopy (SEM). Important differences in the behavior of the nanotubes and the nanowires were observed after the RIE process. The nanotubes remained intact while the nanowires were destroyed by the RIE process. The instability of the peptide nanowires during this process was further confirmed with focused ion beam milling experiments. The PNTS could stand energetic argon ions for around 32 s while the PNWS resisted only 4 s before becoming milled. Based on these results, self-assembled PNTS were further used as an etching mask to fabricate silicon wires in a rapid and low-cost manner. The obtained silicon wires were subjected to structural and electrical characterization by SEM and I–V measurements. Additionally, the fabricated silicon structures were functionalized with fluorescent molecules via a biotin–streptavidin interaction in order to probe their potential in the development of biosensing devices.

Keywords Peptide nanotubes · Peptide nanowires · Self-assembly · Silicon wires · Reactive-ion etching · Masking material · Diphenylalanine

M. B. Larsen · K. B. Andersen · W. E. Svendsen · J. Castillo-León (✉)
Department of Micro and Nanotechnology,
Technical University of Denmark,
Building 345 east, 2800 Kgs,
Lyngby, Denmark
e-mail: jaic@nanotech.dtu.dk
URL: www.nanotech.dtu.dk/Research/nanoSOM/nabis

1 Introduction

Biological nanostructures based on self-assembled peptides have been highlighted as very promising materials for various applications, including drug delivery, electronics, and energy storage, among others [1–3]. Compared to nanomaterials such as carbon nanotubes or silicon nanowires, self-assembled peptides can be fabricated outside the clean room, under mild conditions, and in a rapid, low-cost process [4]. Their preparation in a microfluidic device was recently reported [5]. Diphenylalanine, (FF), the core recognition motif of Alzheimer's β-amyloid peptide, is a short dipeptide that self-assembles into 3D nanostructures (i.e., nanotubes, nanowires, or hydrogels) [4]. The manipulation, electrical and structural characterization, and the stability under liquid conditions of nanotubes formed by FF peptides were recently studied in our group [6–8]. These nanostructures can be easily functionalized [9]; FF nanotubes present extraordinary mechanical properties, and FF nanowires are resistant to thermal, chemical, and proteolytic attacks [10, 11]. All these properties make them promising materials to be used in micro- and nanofabrication processes.

Due to their optical, electrical, photonic, and mechanical properties, silicon wires are extensively used in electronics

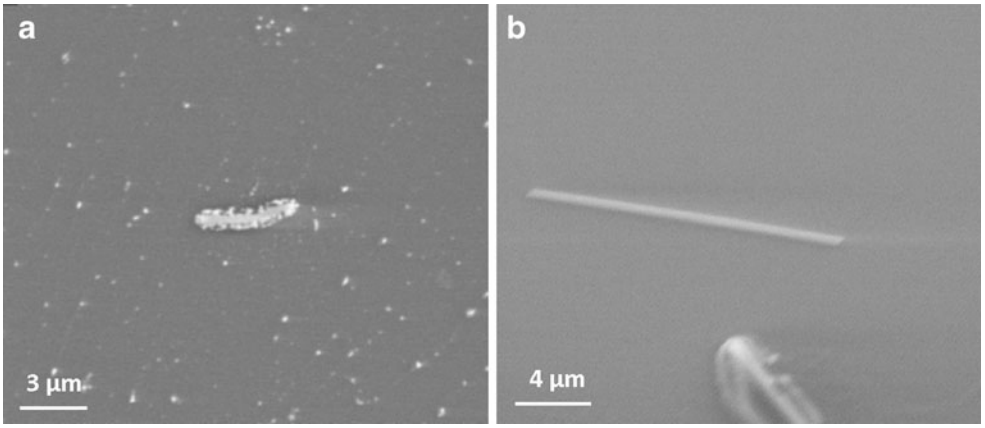

Fig. 1 Comparison of the stability of self-assembled PNWS and PNTS after 1 min under an RIE process. SEM image after RIE of **a** a PNW and **b** a PNT

[12, 13], chemical and biosensor development [14], photonics [15, 16], and microelectromechanical systems [17, 18], among many other applications. Standard techniques for the preparation of silicon wires include top-down and/or bottom-up approaches [19–21]. These methods may include several steps, the use of specialized equipment and in some cases the application of high temperatures and/or pressures [22, 23]. All these conditions increase the fabrication time and costs.

A more simple and low-cost fabrication process that reduces the fabrication time is highly sought after. In this work, peptide nanotubes (PNTS) and peptide nanowires (PNWS) were used as etching mask materials to fabricate silicon wires in a less complicated and low-cost fashion by deep reactive ion etching (RIE). Deep RIE is a powerful top-down fabrication method extensively used to prepare 3D silicon structures [24–31]. The resultant materials were evaluated to prove that functional silicon structures could indeed be obtained using this technique, which thus constitutes a simple, fast, and low-cost method for the preparation of silicon wires.

2 Materials and Methods

Fabrication of self-assembled peptide nanotubes and nanowires Diphenylalanine peptide was purchased from Bachem (cat. no. G-2925, Germany). Fresh stock solutions were prepared by dissolving the lyophilized form of the peptide in 1,1,1,3,3,3-hexafluoro-2-propanol (HFP) (Sigma-Aldrich) at a final concentration of 100 mg/mL. Fresh solutions were prepared before each experiment. Amyloid peptide nanotubes, PNTS, were obtained by dissolving aliquots of a concentrated diphenylalanine peptide stock solution in water.

Peptide nanowires, PNWS, were synthesized following a previously reported method [32]. In short, 10-µL drops of peptide solutions in HFP of concentrations ranging from 0.05

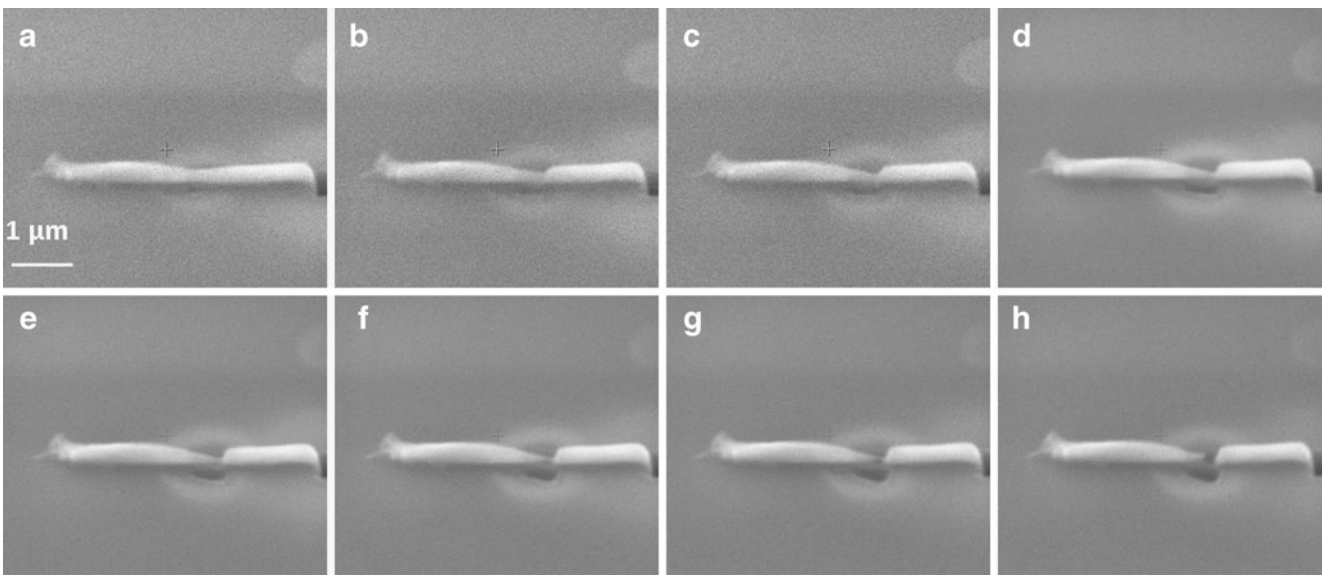

Fig. 2 An SEM image of a PNT being milled using FIB with steps of 2 s; from **a** to **h**

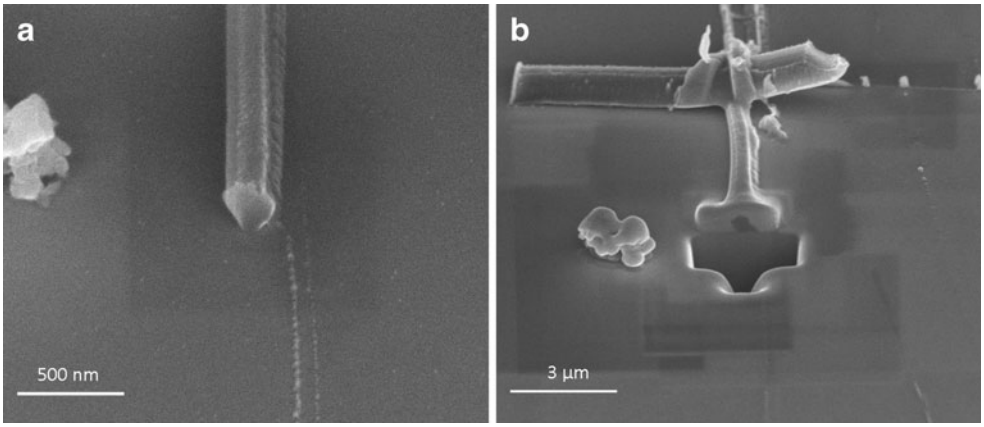

Fig. 3 SEM image of a PNW **a** before and **b** after milling with FIB during 4 s

to 25 mg/mL were pipetted onto the working surface of commercial gold electrodes. The samples were allowed to dry under anhydrous conditions in a vacuum desiccator in order for an amorphous film to form. The aniline vapor treatment was carried out in a Petri dish containing two separate compartments, one for the sample and one for the aniline solvent, in order to allow only the solvent vapor to reach the film. The chamber system was sealed with an aluminum sealing film and placed in the oven for 16 h at 100°C.

Production of polysilicon wafers For the preparation of the polysilicon structures, custom-made silicon nitride SOI wafers, with the insulation layer being silicon nitride, were used. On the wafers, a layer of polysilicon and a layer of insulating silicon nitride, both 100-nm thick, were deposited.

An ultraviolet lithography process was used to define interdigitated electrodes on the surface of the polysilicon wafers. These electrodes were later used as contact pads to connect the fabricated polysilicon structures. A 100-nm aluminum layer was deposited onto the wafers using electron beam evaporation. The remaining aluminum was removed in a lift-off process together with the remained photoresist.

Immobilization of the PNTS and PNWS on the polysilicon wafers The PNTS and PNWS were manually positioned on the polysilicon wafers by placing a droplet of the peptide solution on top of the aluminum electrodes located at their surface.

RIE process An STS C010 Multiplex Cluster System for reactive ion etching was used during this study. During the etching process, SF_6 and O_2 gases with flow rates of respectively 32 standard cubic centimeters per minute (sccm) and 8 sccm were employed. The pressure inside the vacuum chamber was adjusted to 80 mTorr and the RF power to 30 W.

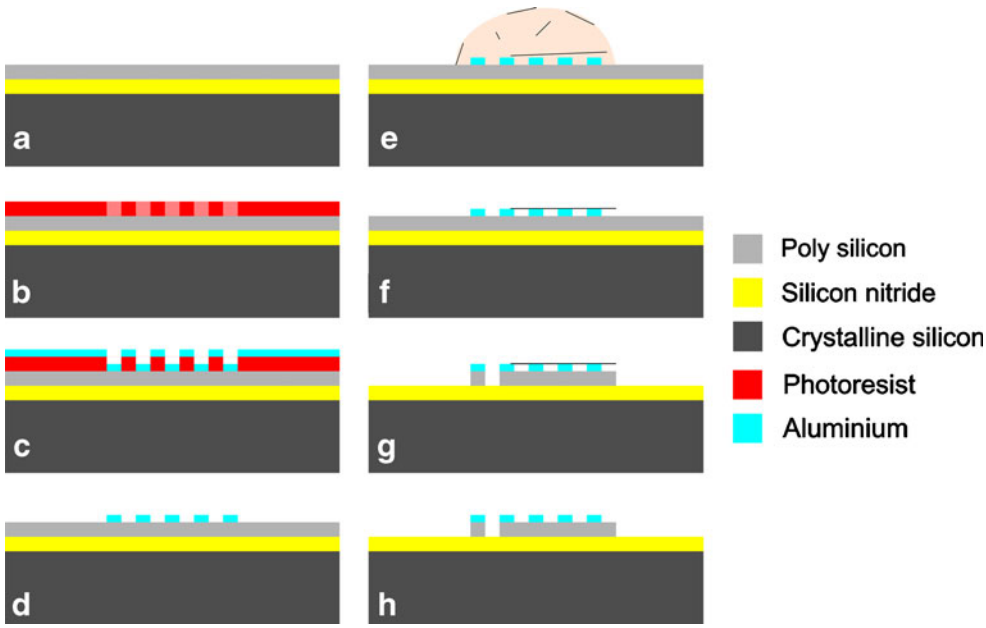

Fig. 4 Process steps for the fabrication of silicon nanostructures using self-assembled peptide nanotubes as an etching mask. **a** 100 nm of polysilicon on a 100-nm silicon nitride wafer. **b–d** Photolithography and metallization steps to define the electrodes. **e–f** Manual peptide tube placement and flushing with DI water. **g** Reactive ion etching of the structures to define the polysilicon wires. **h** Removal of PNTS using distilled water

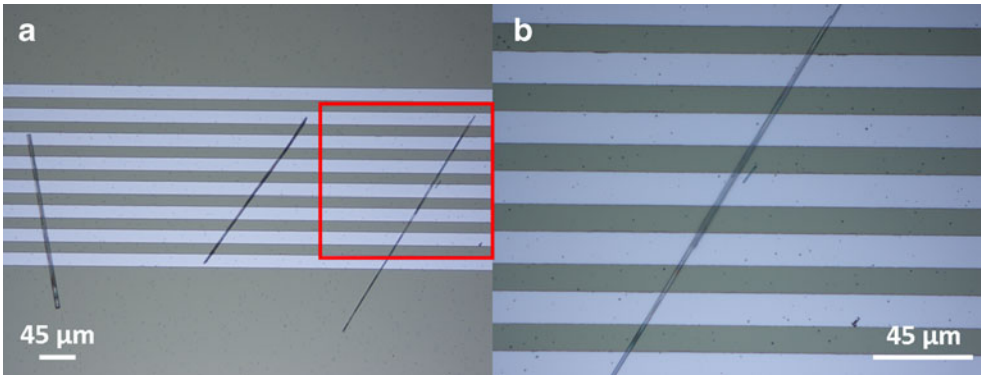

Fig. 5 **a** Optical image of PNTS immobilized on a polysilicon wafer. **b** Zoom of one of the PNTS connecting the aluminum electrodes

Focused Ion Beam For the focused ion beam (FIB) milling experiments on the PNTS and PNWS, a Quanta™ dual-beam scanning electron microscope and focused ion beam work station was utilized. The samples were covered with a layer of gold to avoid charge build up and thus obtain better images and a more precise control during the milling process. The samples were bombarded with Ga ions during several exposure times, after which they were evaluated using scanning electron microscopy (SEM). The milling procedure was conducted in steps of 2 s.

Electrical characterization A current preamplifier (Stanford Research SR570) was used to obtain the I–V curves.

Functionalization of the polysilicon wire The polysilicon wire was thoroughly washed with ethanol to remove any organic contaminant. Subsequently, the wire was immersed in a 2% (3-aminopropyl)triethoxysilane (APTES) ethanol solution for 30 min. The polysilicon wire was washed with ethanol and heated to 120°C for 10 min to completely remove the ethanol. The APTES-modified polysilicon wire was incubated in 1 mg/mL of sulfo-NHS-biotin for 3 h. Following this, the modified wire was incubated with an Atto 610 streptavidin solution during 30 min, and the functionalized wire was finally evaluated using a fluorescent microscope.

3 Results and Discussion

Stability of the self-assembled PNTS and PNWS under RIE The stability of the self-assembled PNTS and PNWS in an RIE process was evaluated. For this, droplets of solutions containing self-assembled tubes and wires were deposited on a silicon wafer and then dried at room temperature. Subsequently, the wafer was placed in the RIE chamber and exposed to the process for 1, 2, and 3 min. At the end of the process, the samples were evaluated using SEM. As shown in Fig. 1, the structure of the self-assembled wires was severely damaged while that of the tubes was unaffected by the RIE process.

This difference in behavior between the two structures, which in this case was attributed to the dissimilarities in their structural conformation, has been previously noted and discussed by other researchers [11]. Ryu and co-workers observed differences in the stability of the same type of self-assembled structures as that investigated in our work when exposed to thermal, chemical, and proteolytic attacks. However, contrary to our findings, the nanowires demonstrated a better resistance to these attacks, and Ryu and co-workers suggested their use in future applications requiring harsh processing conditions. These findings obviously suggest the realization of a more detailed study on the differences in behavior between the two types of

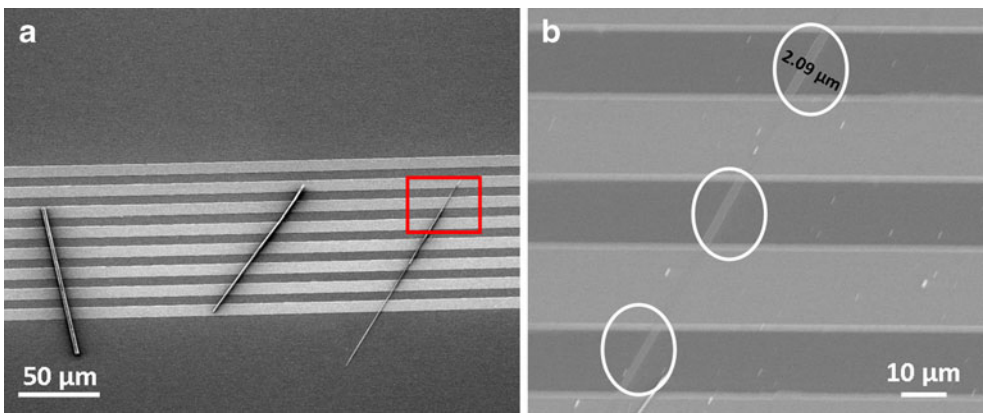

Fig. 6 **a** SEM image of the PNTS located at the surface of the polysilicon wafer. **b** Zoom of the SEM image of the etched silicon wire, inside the *circles*, after removal of the PNTS

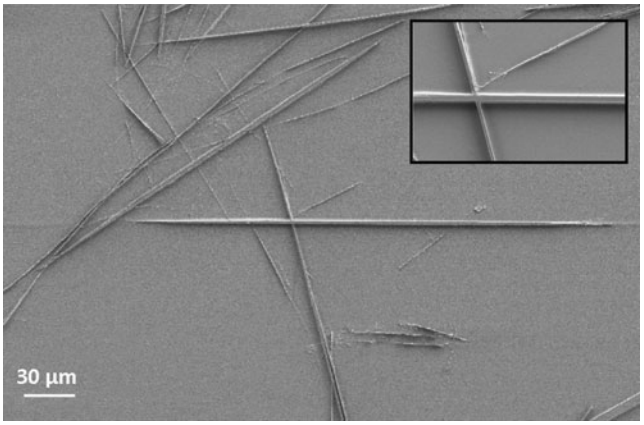

Fig. 7 SEM image of a polysilicon structure etched using two overlapping PNTS. The *inset* displays a zoom of the crossing point where clear ridges can be seen after removal of the PNTS with distilled water

self-assembled peptide structures, which is beyond the goal of the present investigation.

FIB milling FIB milling was used to further confirm the differences in stability between PNTS and PNWS. The FIB technique is very similar to RIE and has previously been used to modify a wide variety of materials, including silicon [33–35]. The obtained results confirmed our previous observations using RIE. PNTS seemed to better resist the bombardment of ions as compared to PNWS. The time required to mill cross-sections of PNTS was longer than the corresponding time for the milling of PNWS. It took 32 s to mill through a peptide nanotube (PNT), cf. Fig. 2, while in the case of the PNW, the same process took only 4 s, cf. Fig. 3.

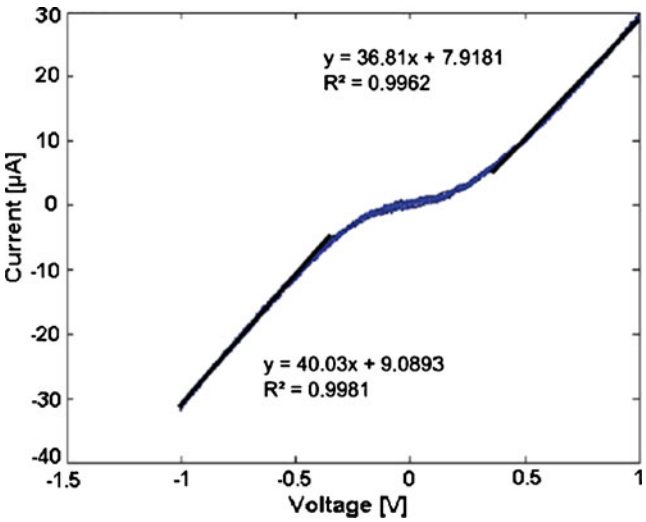

Fig. 8 Characteristic I–V curve of a polysilicon wire fabricated using PNTS as the etching mask material. The voltage was swept from −1 to 1 V. The measured resistance for the negative region was 27.1 MΩ, whereas it was 25.0 MΩ for the positive region

Fabrication of silicon structures using self-assembled PNTS as an etching mask Based on the results from the stability test, self-assembled PNTS were chosen as the etching material for the fabrication of silicon structures in an RIE process. For this, a solution of self-assembled PNTS was manually placed on a silicon wafer containing aluminum electrodes. Once the solvent had been allowed to evaporate at room temperature, the wafer was placed in an RIE chamber and etched for 5 min. The entire process is described in Fig. 4.

An optical image of the PNTS positioned on top of the aluminum electrodes before the RIE process is given in Fig. 5.

Subsequently, the wafer was evaluated with SEM. The PNT was still present after the RIE process, and the structure was found not to be affected by the RIE process, as evidenced in Fig. 6. Figure 6a displays an SEM image of the PNTS after the RIE process. As can be seen, the PNTS were located at the same positions as in Fig. 5, and their structure appeared unaffected by the RIE procedure. Figure 6b displays a zoom of Fig. 6a after removal of the PNT with distilled water. It can be observed that a silicon wire was etched exactly at the same location where the PNT was placed. The fabricated silicon structure displayed the same diameter as the PNT, and it connected the aluminum electrodes on the polysilicon wafer.

Different types of polysilicon structures can be etched based on the initial placement of the PNTS. Figure 7 displays a polysilicon structure etched using two overlapping PNTS as the etching mask. Clear ridges were exposed after rinsing the polysilicon wafer with distilled water to remove the PNTS.

Functionalization and electrical characterization of the etched polysilicon structures In order to evaluate the possibility of employing the fabricated polysilicon structures in the development of biosensing devices, their electrical properties were characterized. For this, an I–V curve was plotted for the etched polysilicon structure connecting the aluminum wires displayed in Fig. 6b. A voltage scan between −1 and 1 V was applied to the aluminum electrodes, and the current through the polysilicon wire connecting the metal electrodes was measured. The obtained I–V curve is given in Fig. 8.

As expected for a conductive silicon structure, the etched polysilicon wire was able to conduct a current after a potential was applied to the metal electrodes. The I–V curve displayed resistances of 27.1 and 25.0 MΩ at the negative and positive regions, respectively. These values indicate that the fabricated polysilicon structure

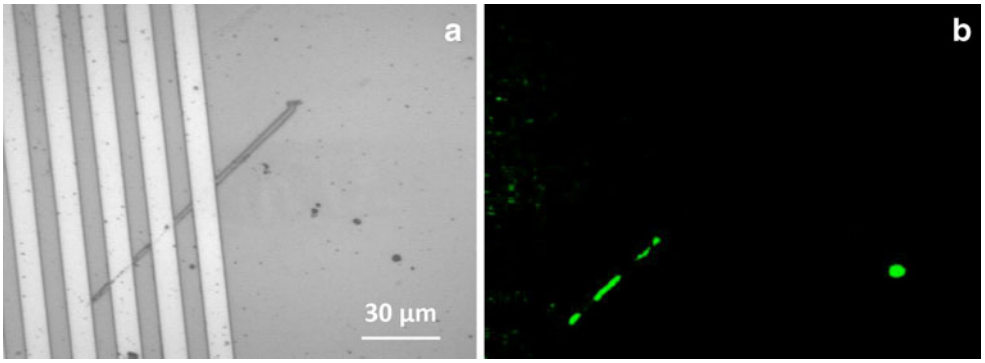

Fig. 9 Optical image of a polysilicon wire fabricated using a self-assembled PNT **a** before the functionalization and **b** after the functionalization with a fluorescent molecule

could be used for the development of a biosensing device such as a field effect transistor or an electrochemical biosensor. The diode behavior for small potential is due to Schottky barriers between the aluminum and the lightly doped polysilicon. In sensor applications, heavy-doped contact regions should be added below the aluminum electrodes.

In order to evaluate the functionalization of the fabricated polysilicon structure, a fluorescent molecule was attached to its surface through the biotin–streptavidin interaction. Figure 9 displays a polysilicon wire before, Fig. 9a, and after, Fig. 9b, the functionalization with Atto 610 streptavidin.

It was found to be possible to attach a fluorescent molecule to the surface of the fabricated polysilicon wire, thus suggesting that the latter could be further functionalized with other functional molecules such as enzymes or antibodies for the development of biosensing devices.

4 Conclusions

Self-assembled PNTS and PNWS were exposed to RIE etching and to an FIB milling process. The self-assembled structures differed in their behavior: the PNTS were more resistant in both cases. These behavioral differences should be further explored in future studies. Nevertheless, based on the obtained results, functional polysilicon wires were fabricated using self-assembled PNTS as an etching mask material. The presented fabrication procedure was fast, simple, and low-cost compared to traditional methods for preparing silicon nanowires. The etched polysilicon structures displayed sizes that were similar to those found when self-assembled PNT were used as an etching mask. Moreover, the conductivity of the fabricated polysilicon structure was evaluated as well as its functionalization through the attachment to a fluorescent molecule. The obtained results suggested that the fabricated polysilicon structure has the potential to be used in the development of biosensing devices.

Acknowledgments The authors would like to thank the European BeNatural project (BeNatural/NMP4-CT-2006-033256) for the financial support and the PhD student Luigi Sasso for the collaboration during the FIB milling experiments.

References

1. de la Rica, R., & Matsui, H. (2010). Applications of peptide and protein-based materials in bionanotechnology. *Chemical Society Reviews, 39*(9), 3499–3509. doi:10.1039/b917574c.
2. Scanlon, S., & Aggeli, A. (2008). Self-assembling peptide nanotubes. *Nano Today, 3*(3–4), 22–30.
3. Yan, X. H., Zhu, P. L., Li, J. B. (2010). Self-assembly and application of diphenylalanine-based nanostructures. *Chemical Society Reviews, 39*(6), 1877–1890. doi:10.1039/b915765b.
4. Reches, M., & Gazit, E. (2006). Designed aromatic homodipeptides: formation of ordered nanostructures and potential nanotechnological applications. *Physical Biology, 3*(1), S10–S19. doi:10.1088/1478-3975/3/1/s02.
5. Castillo-León, J., Rodriguez-Trujillo, R., Gauthier, S., Jensen, A. C. Ø., Svendsen, W. E. (2011). Micro-"factory" for self-assembled peptide nanostructures. *Microelectron Eng*. doi:10.1016/j.mee.2010.12.023.
6. Andersen, K. B., Castillo-Leon, J., Hedstrom, M., Svendsen, W. E. (2011). Stability of diphenylalanine peptide nanotubes in solution. *Nanoscale, 3*(3), 994–998. doi:10.1039/C0NR00734J.
7. Castillo, J., Tanzi, S., Dimaki, M., Svendsen, W. (2008). Manipulation of self-assembly amyloid peptide nanotubes by dielectrophoresis. *Electrophoresis, 29*(24), 5026–5032. doi:10.1002/elps.200800260.
8. Clausen, C. H., Jensen, J., Castillo, J., Dimaki, M., Svendsen, W. E. (2008). Qualitative mapping of structurally different dipeptide nanotubes. *Nano Letters, 8*(11), 4066–4069. doi:10.1021/nl801037k.
9. Reches, M., & Gazit, E. (2007). Biological and chemical decoration of peptide nanostructures via biotin-avidin interactions. *Journal of Nanoscience and Nanotechnology, 7*(7), 2239–2245. doi:10.1166/jnn.2007.645.
10. Diaz, J. A. C., & Cagin, T. (2010). Thermo-mechanical stability and strength of peptide nanostructures from molecular dynamics: self-assembled cyclic peptide nanotubes. *Nanotechnology*. doi:10.1088/0957-4484/21/11/115703.
11. Ryu, J., & Park, C. B. (2009). High stability of self-assembled peptide nanowires against thermal, chemical, and proteolytic

attacks. *Biotechnology and Bioengineering, 105*(2), 221–230. doi:10.1002/bit.22544.
12. Hayden, O., Agarwal, R., Lu, W. (2008). Semiconductor nanowire devices. *Nano Today, 3*(5–6), 12–22.
13. Yang, P., Yan, R., Fardy, M. (2010). Semiconductor nanowire: what's next? *Nano Letters, 10*(5), 1529–1536.
14. Patolsky, F., Zheng, G. F., Lieber, C. M. (2006). Fabrication of silicon nanowire devices for ultrasensitive, label-free, real-time detection of biological and chemical species. *Nature Protocols, 1*(4), 1711–1724. doi:10.1038/nprot.2006.227.
15. Weiss, S. M., & Fauchet, P. M. (2006). Porous silicon one-dimensional photonic crystals for optical signal modulation. *IEEE Journal of Selected Topics in Quantum Electronics, 12*(6), 1514–1519. doi:10.1109/jstqe.2006.884083.
16. Weiss, S. M., Haurylau, M., Fauchet, P. M. (2004). Silicon-based photonic bandgap modulators. In 2004 First IEEE International Conference on Group IV Photonics. pp. 171–173.
17. Arnold, S. P., Prokes, S. M., Zaghloul, M. E. (2005). Localized growth and functionalization of silicon nanowires for MEMS sensor applications. In Oregan, F., Wegemer, C. (Eds.), Proceedings of the 2005 European Conference on Circuit Theory and Design, vol 3. pp. 397–400.
18. Englander, O., Christensen, D., Kim, J., Lin, L. W. (2006). Post-processing techniques for the integration of silicon nanowires and MEMS. In MEMS 2006: 19th IEEE International Conference on Micro Electro Mechanical Systems, Technical Digest. Proceedings: IEEE Micro Electro Mechanical Systems Workshop. pp. 930–933.
19. Bandaru, P. R., & Pichanusakorn, P. (2010). An outline of the synthesis and properties of silicon nanowires. *Semiconductor Science and Technology, 25*(2), 10.1088/0268-1242/25/2/024003.
20. Ozsun, O., Alaca, B. E., Leblebici, Y., Yalcinkaya, A. D., Yildiz, I., Yilmaz, M., et al. (2009). Monolithic integration of silicon nanowires with a microgripper. *Journal of Microelectronic Systems, 18*(6), 1335–1344. doi:10.1109/jmems.2009.2034340.
21. Weber, J., Singhal, R., Zekri, S., Kumar, A. (2008). One-dimensional nanostructures: fabrication, characterisation and applications. *International Materials Reviews, 53*(4), 235–255. doi:10.1179/174328008x348183.
22. Colli, A., Fasoli, A., Pisana, S., Fu, Y., Beecher, P., Milne, W. I., et al. (2008). Nanowire lithography on silicon. *Nano Letters, 8*(5), 1358–1362. doi:10.1021/nl080033t.
23. Fellahi, O., Hadjersi, T., Maamache, M., Bouanik, S., Manseri, A. (2010). Effect of temperature and silicon resistivity on the elaboration of silicon nanowires by electroless etching. *Applied Surface Science, 257*(2), 591–595. doi:10.1016/j.apsusc.2010.07.039.
24. Abe, H., Yoneda, M., Fujlwara, N. (2008). Developments of plasma etching technology for fabricating semiconductor devices. *Japanese Journal of Applied Physics, 47*(3), 1435–1455. doi:10.1143/jjap.47.1435.
25. Barlian, A. A., Park, W. T., Mallon, J. R., Rastegar, A. J., Pruitt, B. L. (2009). Review: semiconductor piezoresistance for microsystems. *Proceedings of the IEEE, 97*(3), 513–552.
26. Esashi, M., & Ono, T. (2005). From MEMS to nanomachine. *Journal of Physics. D. Applied Physics, 38*(13), R223–R230. doi:10.1088/0022-3727/38/13/r01.
27. Fu, Y. Q., Colli, A., Fasoli, A., Luo, J. K., Flewitt, A. J., Ferrari, A. C., et al. (2009). Deep reactive ion etching as a tool for nanostructure fabrication. *Journal of Vacuum Science and Technology B, 27*(3), 1520–1526. doi:10.1116/1.3065991.
28. Han, X. L., Larrieu, G., Dubois, E. (2010). Realization of vertical silicon nanowire networks with an ultra high density using a top-down approach. *Journal of Nanoscience and Nanotechnology, 10*(11), 7423–7427. doi:10.1166/jnn.2010.2841.
29. Hirai, Y., Yabu, H., Matsuo, Y., Ijiro, K., Shimomura, M. (2010). Biomimetic bi-functional silicon nanospike-array structures prepared by using self-organized honeycomb templates and reactive ion etching. *Journal of Materials Chemistry, 20*(48), 10804–10808. doi:10.1039/c0jm02423f.
30. Mehran, M., Sanaee, Z., Mohajerzadeh, S. (2010). Formation of silicon nanograss and microstructures on silicon using deep reactive ion etching. *Micro and Nano Letters, 5*(6), 374–378. doi:10.1049/mnl.2010.0111.
31. Strobel, S., Kirkendall, C., Chang, J. B., Berggren, K. K. (2010). Sub-10 nm structures on silicon by thermal dewetting of platinum. *Nanotechnology, 21*(50), 7. doi:10.1088/0957-4484/21/50/505301.
32. Ryu, J., & Park, C. B. (2008). High-temperature self-assembly of peptides into vertically well-aligned nanowires by aniline vapor. *Advanced Materials, 20*(19), 3754–3758.
33. Giannuzzi, L. A., & Stevie, F. A. (1999). A review of focused ion beam milling techniques for TEM specimen preparation. *Micron, 30*(3), 197–204.
34. Korotcenkov, G., & Cho, B. K. (2010). Silicon porosification: state of the art. *Critical Reviews in Solid State and Materials Sciences, 35*(3), 153–260. doi:10.1080/10408436.2010.495446.
35. Tseng, A. A. (2004). Recent developments in micromilling using focused ion beam technology. *Journal of Micromechanics and Microengineering, 14*(4), R15–R34. doi:10.1088/0960-1317/14/4/ro1.